

The temperature dependence of bytownite feldspar dissolution in neutral aqueous solutions of inorganic and organic ligands at low temperature (5–35°C)

Susan A. Welch^{a,b,*}, William J. Ullman^{b,1}

^a Department of Geology and Geophysics, University of Wisconsin-Madison, Lewis G. Weeks Hall, 1215 West Dayton St., Madison, WI 53706, USA

^b College of Marine Studies, University of Delaware, 700 Pilottown Rd., Lewes, DE 19958, USA

Received 19 October 1998; accepted 21 November 1999

Abstract

The temperature dependence of silica release from bytownite, a Ca–Al-rich feldspar, was determined in solutions of inorganic and organic ligands at neutral pH from 5°C to 35°C. The apparent activation energy of dissolution in the inorganic (distilled water and KNO₃) solutions was approximately 10 kcal/mol. The rates and temperature dependence of dissolution in acetate solutions were indistinguishable from those in the inorganic solutions. In contrast, both oxalate and gluconate enhanced the dissolution of the feldspar framework relative to the KNO₃ and distilled water controls, presumably by catalyzing Al release from the mineral surface. The apparent activation energy of Si release from feldspar in the oxalate and gluconate solutions was approximately 7 kcal/mol and is due primarily to the larger enhancement of dissolution rates at low temperature. While the catalytic impact of complexing organic ligands on mineral dissolution is clear, this mechanism alone cannot be responsible for the observed biotic enhancement of weathering in field situations. © 2000 Elsevier Science B.V. All rights reserved.

Keywords: Temperature dependence; Bytownite feldspar dissolution; Ligands

1. Introduction

The chemical weathering of Ca- and Mg-silicate minerals is an important component of the feedback

mechanism controlling atmospheric CO₂ concentrations and, therefore, global climate (Walker et al., 1981; Berner et al., 1983). The dissolution of these minerals in continental settings releases Ca and Mg ions to solution, which react, primarily in the ocean, to produce and deposit sedimentary Ca- and Mg-carbonates, thereby regulating CO₂ concentration in the ocean and atmosphere. At higher temperatures, continental weathering rates and the flux of Ca and Mg to the ocean increase; as a consequence, the flux of CO₂ from the atmosphere to marine sediments increases. Knowledge of the mechanisms and tem-

* Corresponding author. Department of Geology and Geophysics, University of Wisconsin-Madison, Lewis G. Weeks Hall, 1215 West Dayton St., Madison, WI 53706, USA. Tel.: +1-608-262-0915; fax: +1-608-262-0693.

E-mail address: swelch@geology.wisc.edu (S.A. Welch).

¹ Tel.: +1-302-645-4302; fax: +1-302-645-4007.

perature behavior of weathering reactions is, therefore, an important input into predictive models of global climate change (Berner et al., 1983; Brady, 1991).

The impact of this feedback mechanism is dependent on the overall temperature dependence of the weathering reactions. This temperature dependence is usually described as an apparent activation energy and is expressed using the Arrhenius equation:

$$k = Ae^{-\left(\frac{E_a}{RT}\right)}, \quad (1)$$

where k is the rate constant, A is a preexponential factor, E_a is the apparent activation energy of the reaction, R is the ideal gas constant and T is absolute temperature. At higher values of E_a , the feedback between reaction rate and temperature and the ability of weathering to control atmospheric CO_2 is greater (Brady, 1991; Brady and Carroll, 1994). While the Arrhenius relationship, in principle, describes the temperature dependence of only elementary reactions, the close fit of a large number of biogeochemical reactions, including mineral dissolution, to this model argues that many of these reactions have a single important rate-controlling step.

The apparent activation energy for silicate mineral dissolution has been estimated from both field and laboratory measurements. Velbel (1993) used stream water chemistry to calculate a value of 18.4 kcal/mol for apparent activation energy of mineral dissolution in the field. A slightly higher value, 26.2 kcal/mol, was estimated by Dorn and Brady (1995), who compared microscopic dissolution features on plagioclase feldspar minerals from basalt flows at different altitudes in Hawaii.

Laboratory estimates of E_a for silicate minerals range from 1 to 30 kcal/mol with most values falling in the 10 to 20 kcal/mol range (Brady, 1991; Brady and Carroll, 1994; Wogelius and Walther, 1991; Hellmann, 1994; Lasaga et al., 1994 and references therein). Most of these experiments have focused on weathering reactions at higher temperatures, i.e., from room temperature to hydrothermal or formation water temperature (≈ 25 – 300°C). There is less direct information on the effects of temperature on mineral dissolution rates at lower temperatures. This lower range of temperature (≈ 0 – 25°C) is important, however, since continental weathering oc-

curs predominately in these low-temperature environments. In these environments, biological production of both organic and inorganic acids may influence the mechanism of reaction, may enhance mineral dissolution rates in ways unanticipated by the high temperature experiments and may, therefore, moderate the feedback between mineral weathering and climate in ways not currently understood (Brady et al., 1999).

The purpose of this study is to determine the temperature dependence of the dissolution of a Ca–Al-rich feldspar (bytownite) at near-neutral pH from 5°C to 35°C . Experiments were conducted in short-duration batch reactors in which Si release was used as a proxy for overall feldspar dissolution rates, even though stoichiometric dissolution was neither expected nor attained (Casey and Bunker, 1990). Batch reactors were chosen because they allow easy replication and comparison to other experiments, which were performed in our laboratory (Welch and Ullman, 1999). We assume that the mechanism of silica release in short-duration experiments is the same as in long-duration experiments and, therefore, the activation energy should be the same. Other investigators have performed long-duration (thousands of hours) flow-through experiments that yield similar overall reaction rates to the ones measured here, but may be more appropriate for determining the pre-exponential factor A in Eq. 1 (Stillings and Brantley, 1995; Stillings et al., 1996; Chen and Brantley, 1997). Short-duration experiments (< 360 h) were chosen as they were sufficiently long to permit linear release rates to be measured after the initial equilibration of the solid with the reactive solution and sufficiently short to minimize the impact of chemical affinity on rate determinations. Si-release rates were used as a proxy for overall dissolution rates as the breakdown of the feldspar (Si, Al) framework is the mechanism controlling long-term dissolution rates, and the other framework element, Al, is subject to a wide variety of secondary reactions.

The temperature dependence of dissolution was determined for feldspars dissolved in solutions of both inorganic and organic ligands to determine the possible effects of microbial metabolites on the apparent activation energy of feldspar dissolution. Distilled water and KNO_3 solutions were used as inorganic controls to determine the hydrolytic dissolution

rate. Acetate and oxalate were chosen as representative organic acids because they are produced by a variety of plants and microorganisms and are among the most abundant organic acids found in natural systems (Graustein et al., 1977; Fisher, 1987; Fox and Comerford, 1990). Both of these compounds enhance mineral dissolution rates in laboratory experiments (Surdam et al., 1984; Manley and Evans, 1986; Mast and Drever, 1987; Welch and Ullman, 1993; Franklin et al., 1994; Stillings et al., 1996) presumably by catalyzing Al release from the mineral surface. Gluconate was also used in these experiments as it is the most abundant low molecular-weight organic ligand produced by several naturally occurring subsurface bacteria used in mineral dissolution experiments in our laboratory in which enhanced dissolution rates were observed (Vandevivere et al., 1994; Welch, 1996).

2. Materials and methods

2.1. Solids

Crystal Bay (Minnesota) bytownite (Wards Scientific Establishment, Rochester, NY), a Ca–Al-rich member of the plagioclase series, was chosen for these experiments. This feldspar was used in previous experiments in our laboratory (Ullman et al., 1996; Welch and Ullman, 1996), has a fairly homogeneous composition, and is nearly free of impurities. Samples with extensive weathering rinds or visible mineral impurities were discarded. The remaining samples were crushed to a particle size of less than 1 mm. The 125–250 μm size fraction (collected by sieving) was used for these experiments. Before the experiments, the feldspar sand was washed approximately 50 times with deionized water until the supernatant was clear and then dried at 110°C for several hours. Iron filings introduced in the crushing procedure and magnetic minerals were removed using a magnet and a Frantz Isodynamic Magnetic Separator. To remove the remaining fines and any very reactive material which can cause rapid and variable initial dissolution behavior (Welch and Ullman, 1993), the feldspar sand was further washed with 0.1 mM HCl for several hours and rinsed again with deionized water. This treatment was not ex-

pected to significantly alter mineral surface chemistry since dissolution of the major framework ions is approximately stoichiometric at this pH (Welch and Ullman, 1993). Initial surface area as determined by Kr-gas BET was 0.0815 m^2/g (Lowell and Shields, 1984). The composition of bytownite from this locality was determined by X-ray fluorescence (Xral, Toronto) and is approximately $\text{K}_{0.01}\text{Na}_{0.23}\text{Ca}_{0.77}\text{Al}_{1.75}\text{Si}_{2.25}\text{O}_8$.

2.2. Solutions

Solutions were prepared by dissolving reagent grade chemicals in Si-free deionized water. Bytownite feldspar was dissolved in deionized water and in 1 mM solutions of potassium nitrate, sodium acetate, sodium oxalate and sodium gluconate. The deionized water (saturated with air) and the KNO_3 solution were chosen to demonstrate the temperature dependence of hydrolytic dissolution at neutral pH and to serve as controls for the organic ligand experiments. Acetate represents the class of organic ligands that only weakly complex dissolved Al and only slightly enhanced dissolution rates at low temperatures. Oxalate and gluconate represent the class of ligands that strongly complex dissolved Al and strongly enhance feldspar dissolution rates. Distilled water was used without further pH adjustment. The initial pH of the remaining solutions was adjusted to between 6 and 6.5, which is at the lower end of the range where mineral dissolution rates are lowest and essentially independent of pH (Chou and Wollast, 1985; Blum and Lasaga, 1988; Brady and Walther, 1989; Welch and Ullman, 1993). The pHs of these experiments were expected to drift toward the neutral range, although the buffering capacity of the solutions in equilibrium with atmospheric carbon dioxide was expected to minimize this drift. In all cases, pHs remained in the pH independent dissolution range. With the exception of the distilled water controls, the final experimental pHs were in the range of 6.0 ± 0.2 . The final pH of the distilled water controls were 6.5 ± 0.3 .

2.3. Experimental

Two grams of clean feldspar sand were added to 100 ml of solution in an acid-washed polycarbonate

batch reactor. Three replicate experiments were conducted for each treatment: deionized water, potassium nitrate, sodium acetate, sodium oxalate and sodium gluconate. Bottles were placed on a shaker table (100 rpm) in an incubator maintained within 0.5°C of the experimental temperatures (5°C, 20°C and 35°C). Five-milliliter aliquots of solution were removed daily from each bottle for the first 3 days of the experiment and then every other day for the next 12 days. Dissolved Si, dissolved Al and pH were determined for each aliquot sample. The pH was determined potentiometrically with reference to commercial NBS buffers. Dissolved Si concentration was determined using the silico-molybdenum blue method using a Perstorp Flo-Solution automated wet chemical analyzer. The detection limit for this method is approximately 0.05 μM Si. Dissolved Al was determined by ion chromatography using lumogallion as a post-column reagent and fluorescence detection. This method can detect and distinguish between free (or weakly complexed) and strongly complexed Al in solution and has a detection limit of approximately 0.3 μM Al.

Accumulated Si-release is determined from measured Si concentrations in solution according to the following formula:

$$m(t) = m(t-1) + (c(t) - c(t-1))V(t-1),$$

where $m(t)$ and $m(t-1)$ are the accumulated mass of silica released at the end of the t and $t-1$ intervals, $c(t)$ and $c(t-1)$ are the concentrations of silica found in solution at the end of the t and $t-1$ intervals and $V(t-1)$ is the amount of solution remaining in the reactor after the sample was removed at the $t-1$ interval. The slope of $m(t)$, normalized to initial surface area, vs. t yields the silica release rate.

3. Results

3.1. Feldspar dissolution in inorganic solutions

The average silica release (mean and standard deviation of three replicate reactors, normalized to initial surface area and taking into account the volume changes due to sample removal) for the two inorganic controls is plotted vs. time in Fig. 1. The

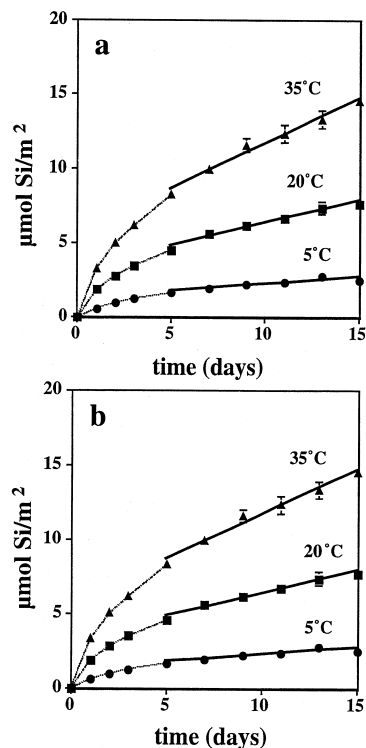


Fig. 1. Si release normalized to the initial surface area for feldspar dissolved in (a) deionized water and (b) potassium nitrate at 5°C (●), 20°C (■) and 35°C (▲). Dissolution rate was calculated from a linear fit of the data from day 5 to day 15.

slope of the curve is the instantaneous Si-release rate. In all of the inorganic experiments, Si release was more rapid in the first few days, but was slower and approximately constant after 5 days. Overall dissolution rates were, therefore, determined from a linear fit of the Si release curve from day 5 through day 15. Dissolution rates increased from approximately 0.1 to 0.6 $\mu\text{mol Si/m}^2/\text{day}$ as temperatures increased from 5°C to 35°C (Table 1). Rates were slightly, but not significantly, lower in the KNO_3 treatment than in the deionized water treatment, indicating that there may be a small inhibition of dissolution due to the effects of ionic strength (Stillings and Brantley, 1995). Dissolved aluminum release was not detected in these experiments.

3.2. Feldspar dissolution in organic acid solutions

The results of feldspar dissolution experiments in 1 mM acetate solutions were very similar to the

Table 1
Silica release rates ($\mu\text{mol}/\text{m}^2/\text{day}$) from bytownite feldspar and apparent activation energies of bytownite dissolution^a

Temperature (°C)	DI	KNO ₃	Acetate	Oxalate	Gluconate
5	0.117 ± 0.025	0.107 ± 0.025	0.107 ± 0.011	0.268 ± 0.031	0.151 ± 0.014
	0.121 ± 0.029	0.096 ± 0.014	0.097 ± 0.010	0.193 ± 0.059	0.168 ± 0.015
	0.114 ± 0.032	0.088 ± 0.025	0.079 ± 0.015	0.257 ± 0.044	0.152 ± 0.010
Mean	0.118 ± 0.003	0.097 ± 0.009	0.095 ± 0.014	0.239 ± 0.041	0.157 ± 0.010
20	0.301 ± 0.025	0.305 ± 0.024	0.357 ± 0.021	0.488 ± 0.042	0.380 ± 0.045
	0.420 ± 0.054	0.324 ± 0.042	0.321 ± 0.014	0.628 ± 0.021	0.362 ± 0.056
	0.298 ± 0.026	0.291 ± 0.025	0.310 ± 0.019	0.401 ± 0.092	0.314 ± 0.015
Mean	0.340 ± 0.070	0.307 ± 0.016	0.329 ± 0.025	0.506 ± 0.114	0.352 ± 0.034
35	0.654 ± 0.048	0.570 ± 0.032	0.604 ± 0.047	0.594 ± 0.059	0.595 ± 0.020
	0.634 ± 0.050	0.692 ± 0.056	0.624 ± 0.056	0.996 ± 0.111	0.556 ± 0.036
	0.632 ± 0.050	0.542 ± 0.056	0.641 ± 0.065	0.702 ± 0.041	0.482 ± 0.047
Mean	0.640 ± 0.012	0.601 ± 0.080	0.623 ± 0.018	0.764 ± 0.208	0.544 ± 0.057
E_a (kcal/mol)	9.7	10.4	10.8	6.6	7.1
Standard error	± 0.6	± 0.6	± 0.8	± 1.0	± 0.5
95% confidence interval	± 1.5	± 1.5	± 1.8	± 2.4	± 1.3

^aReplicate determinations of release rate (\pm standard deviation) are given together with the mean release rate for each treatment. For the E_a determinations, both the standard error, determined from the analysis of covariance, and the 95% confidence interval ($df = 7$) are given.

inorganic controls at all three temperatures (Table 1 and Fig. 2a). The initial Si-release rate was rapid but then decreased and became more constant after several days. There was no significant enhancement of dissolution rate in the acetate solution, compared to the inorganic controls (Table 1), and as in the controls; there was no detectable Al release to solution.

Silica release from feldspars dissolved in oxalic acid at neutral pH follows a similar trend as in the inorganic controls. However, Si release was significantly greater in the oxalate solutions than in the controls (Table 1 and Fig. 2b). The relative increase in dissolution was dependent on temperature. Silica release was approximately 150% higher in the oxalate solution than in the nitrate solution at 5°C, 65% higher at 20°C and 27% higher at 35°C. The higher Si-release rates correspond to the higher Al-release rates (Fig. 2d) and is consistent with the previously advanced hypothesis that feldspar dissolution rates are catalyzed by the interaction of ligands with Al sites on the mineral surface followed by Al release to solution (Welch and Ullman, 1993). Based on the chromatographic separation of the Al peaks, most of the dissolved Al was present as Al–oxalate complexes; free Al³⁺ or its hydrolysis products were not detected in most of the samples analyzed. Dissolu-

tion rates determined from the slope of the Si-release curves from day 5 to day 15 and ranged from 0.24 $\mu\text{mol Si}/\text{m}^2/\text{day}$ at 5°C to 0.76 $\mu\text{mol Si}/\text{m}^2/\text{day}$ at 35°C (Table 1).

Silica release from bytownite in gluconate solutions is plotted in Fig. 2c. Silica release rates are slightly enhanced in the gluconate solutions compared to the KNO₃ controls at 5°C and 20°C (Table 1 and Fig. 2c). Dissolution rate was slightly but not significantly lower at 35°C in gluconate ($0.544 \pm 0.05 \mu\text{mol Si}/\text{m}^2/\text{day}$) compared to the KNO₃ control ($0.601 \pm 0.080 \mu\text{mol Si}/\text{m}^2/\text{day}$), indicating that dissolution is perhaps slightly inhibited in gluconate solutions at this temperature. As in the oxalate experiment, Al release is highest at the lower temperatures (Fig. 2e). In contrast to the observations in the oxalate experiments, the chromatographic evidence suggests that the dissolved Al was present as free, hydrolyzed or weakly complexed Al.

4. Discussion

4.1. Short-duration batch experiments

The short-duration experiments used to determine the temperature dependence of bytownite dissolution

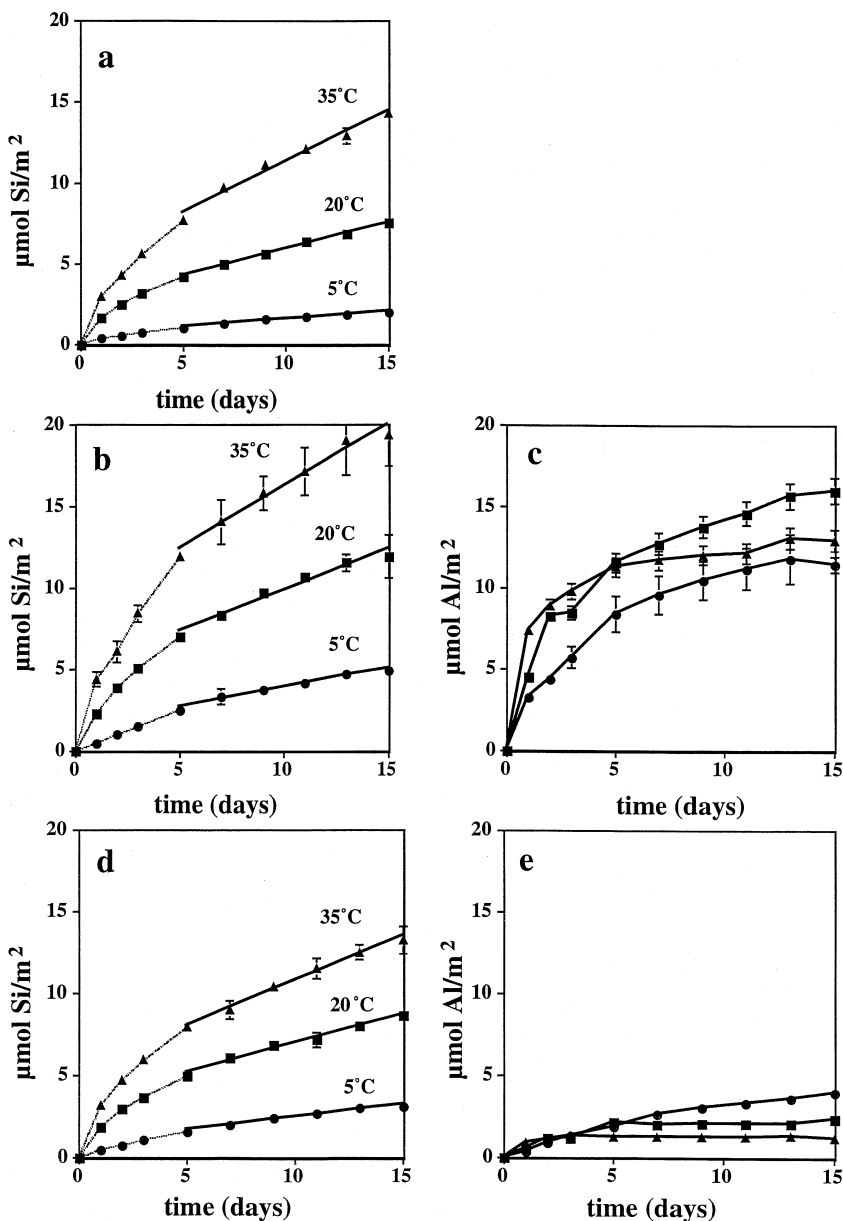


Fig. 2. Si and Al release normalized to the initial surface area for feldspar dissolved at 5°C (●), 20°C (■) and 35°C (▲). (a) Si release in 1 mM sodium acetate (no Al detected). (b) Si and (c) Al release in 1 mM oxalate. (d) Si and (e) Al release in 1 mM sodium gluconate. Dissolution rate based on Si release was calculated from a linear fit of the data from day 5 to day 15.

are not the ideal experiment to determine the long-term steady-state dissolution rates that may be more appropriate for inferring the rates of mineral weathering in the field. Nonetheless, these experiments give useful results for the purpose of determining the

temperature dependence of the dissolution reaction and the role of ligands in the dissolution process.

The feldspar dissolution rates determined in inorganic solutions in batch reactors ranged from approximately 0.1–0.6 $\mu\text{mol Si/m}^2/\text{day}$ or 1.2×10^{-12} –

7×10^{-12} mol Si/m²/s. These rates are within an order of magnitude of the dissolution rates determined for bytownite in flow-through reactors in our laboratory using similar solutions and in the same range as rates determined by other studies under similar experimental conditions (Stillings et al., 1996, Welch and Ullman, 1996, and references therein). Si-release rates were enhanced in solutions of complexing organic acids, oxalate and gluconate, by a factor of 15% to 150% compared to inorganic and noncomplexing control solutions. This is considerably less than what was observed for the dissolution of bytownite in similar conditions in flow-through reactors where dissolution rates were enhanced by as much as an order of magnitude (Welch and Ullman, 1993; Vandevivere et al., 1994), but still represents a significant effect.

4.1.1. Time dependence of reaction

Si release (Figs. 1 and 2) was most rapid in the first few days of the experiments and then decreased and became approximately linear with time. This initial rapid dissolution (so-called ‘parabolic’) phase has been observed in many mineral dissolution experiments and has been attributed to a variety of processes. The rapid initial dissolution rates is most likely an artifact of the mineral crushing procedure which creates strained sites, cracks, distortions, and fine particles, all of which could be sites of preferential dissolution (Berner and Holdren, 1979; Eggleston et al., 1989). The mineral pretreatment (water and weak acid washing) should remove most, though possibly not all, of these experimental artifacts. High initial rates could also be caused by the formation of a leached layer on the fresh mineral surface (Chou and Wollast, 1984, 1985) or rapid dissolution of the primary mineral phase followed by slower precipitation of a secondary phase (Holdren and Addams, 1982). The nonstoichiometric dissolution could support either the leached layer or secondary precipitate hypothesis, although there has not been sufficient reaction in these experiments to create a detectable diffusion-inhibiting leached layer over the entire mineral surface. The total amount of Si released from the feldspar in any of our experiments corresponds to the dissolution of less than one unit cell thickness over the initial available mineral surface. The slower and more constant Si-release rate after

the initial 5 days was used to calculate apparent feldspar dissolution rates and the temperature dependence of dissolution.

4.1.2. Chemical affinity and secondary precipitation

The rate of the bytownite dissolution reaction may be a function of the solution saturation state with respect to the primary mineral even well away from equilibrium conditions (Nagy and Lasaga, 1992; Nagy et al., 1991; Burch et al., 1993). In experiments with the Na–Si-rich member of the plagioclase series, albite, Burch et al. (1993) found that dissolution rates decreased in response to solution composition when the chemical affinity, $\Delta G_r = RT \ln(Q/K)$, where Q is the ion activity product and K is the equilibrium constant for the homogenous dissolution reaction, was greater than -10 kcal/mol. The critical chemical affinity for gibbsite was -0.5 kcal/mol and for kaolinite was -2 kcal/mol (Nagy and Lasaga, 1992; Nagy et al., 1991). Our experiments were designed to remain on the ‘dissolution plateau’ below the critical value of ΔG_r for bytownite dissolution, where rates are independent of chemical affinity, although the value for this mineral is not known. The approximately linear Si-release rates observed in our experiments after the first 5 days provides experimental confirmation that the chemical affinity effect can be neglected.

Another concern is the possibility of secondary precipitation of Si-containing phases that would affect the reliability of our estimated bytownite dissolution rates. We anticipated that Al phases (most likely gibbsite, Al(OH)₃) would precipitate in some solutions but hoped to avoid the precipitation of mixed Al–Si clays, such as kaolinite, in our experiments. Again, the constant Si-release rate from 5 to 15 days provides experimental evidence that secondary precipitation of Si-containing phases cannot be an important effect: either aluminum-silicate secondary phases are not being precipitated, or the rate at which they are precipitating is slow enough as to be neglected.

The impact of the chemical affinity on dissolution and precipitation can be further addressed using an ion association thermodynamic model. PHREEQC (Version 1.6, 20 May 1998, Parkhurst, 1995) was used together with additional thermodynamic data (Table 2) to estimate the saturation indices with

Table 2
Thermodynamic data used in equilibrium calculations

Reaction ^a	log k	ΔH (kJ/mol)	Source or compilation ^b
$\text{Ox}^{2-} + \text{H}^+ \rightarrow \text{HOx}^-$	4.266	4.43	Smith and Martell (1993), and references therein
$\text{Ox}^{2-} + 2\text{H}^+ \rightarrow \text{H}_2\text{Ox}^-$	5.518	10.04	Smith and Martell (1993) (from tabulated stepwise reactions)
$\text{Ox}^{2-} + \text{Na}^+ \rightarrow \text{NaOx}^-$	1.0	5.02	Smith and Martell (1993), and references therein
$\text{Ox}^{2-} + \text{Ca}^{2+} \rightarrow \text{CaOx}$	3.19	0 ^c	
$\text{Ox}^{2-} + \text{Al}^{3+} \rightarrow \text{AlOx}^+$	7.34	0 ^c	Mean of values from Bottari and Ciavatta (1968), Gordienko and Mikhailyuk (1970), Jaber et al. (1977) and Sjöberg and Öhman (1985)
$2\text{Ox}^{2-} + \text{Al}^{3+} \rightarrow \text{AlOx}_2^-$	13.08	0 ^c	Mean of values from Bottari and Ciavatta (1968), Jaber et al. (1977) and Sjöberg and Öhman (1985)
$3\text{Ox}^{2-} + \text{Al}^{3+} \rightarrow \text{AlOx}_3^{3-}$	16.78	0 ^c	Jaber et al. (1977) and Sjöberg and Öhman (1985)
$\text{Gl}^- + \text{H}^+ \rightarrow \text{HGl}$	3.72	0 ^c	Motekaitis and Martell (1984) (average of two values)
$\text{Gl}^- + \text{Ca}^{2+} \rightarrow \text{CaGl}^+$	1.55	0 ^c	Masone and Vicedomini (1981) (average of two values)
$\text{Gl}^- + \text{Al}^{3+} \rightarrow \text{AlGl}^{2+}$	2.56	0 ^c	Motekaitis and Martell (1984) (mixed complexes are equivalent to $\text{AlH}_{-1}\text{Gl}^+$ and $\text{AlH}_{-3}\text{Gl}^-$ reported by these investigators with water equilibrium added)
$\text{Gl}^- + \text{Al}^{3+} + \text{OH}^- \rightarrow \text{AlOHGl}^+$	13.97	0 ^c	
$\text{Gl}^- + \text{Al}^{3+} + 3\text{OH}^- \rightarrow \text{Al}(\text{OH})_3\text{Gl}^-$	32.46	0 ^c	
$\text{Ac}^- + \text{H}^+ \rightarrow \text{HAc}$	4.757	0.41	Smith and Martell (1993), and references therein
$\text{Ac}^- + \text{Na}^+ \rightarrow \text{NaAc}$	-0.18	12.6 ^d	
$\text{Ac}^- + \text{Ca}^{2+} \rightarrow \text{CaAc}^+$	1.18	4 ^d	
$\text{Ac}^- + \text{Al}^{3+} \rightarrow \text{AlAc}^{2+}$	2.75	0 ^c	Palmer and Bell (1994)
$2\text{Ac}^- + \text{Al}^{3+} \rightarrow \text{Al}(\text{Ac})_2^+$	7.35	0 ^c	
Bytownite (Crystal Bay) $\text{Na}_{0.25}\text{Ca}_{0.75}\text{Al}_{1.75}\text{Si}_{2.25}\text{O}_8$ + $8\text{H}_2\text{O} \rightarrow 0.25\text{Na}^+ + 0.75\text{Ca}^{2+}$ + $1.75\text{Al}(\text{OH})_4^- + 2.25\text{H}_4\text{SiO}_4$	-19.29	63.42	Parkhurst (1995) (linear interpolation between anorthite and albite end-members in database)

^aOx = oxalate = $\text{C}_2\text{O}_4^{2-}$; Ac = acetate = CH_3COO^- ; Gl = gluconate = $\text{C}_5\text{H}_{11}\text{O}_5\text{COO}^-$.

^bReferences found in Smith and Martell (1993) and Nordstrom and May (1996). Data extrapolated to $I = 0$ as needed.

^cNo enthalpy found: $H_f = 0$ assumed.

^dQuestionable value used.

respect to both the primary bytownite and potential secondary phases at the end of each experiment. The data used (Ca, Al and Na were, in some cases, estimated) and results of these calculations are given in Table 3. These calculations indicate that at no time in our experiments were the experimental solutions saturated with respect to amorphous silica or kaolinite, the most likely Si-containing secondary phases, and that the solutions were always significantly undersaturated with respect to the primary bytownite ($\Delta G_r = -15.8$ to -24.5 kcal/mol). Although our estimates of Ca concentrations may reflect only a minimum concentration (Ca release from feldspars often exceeds the stoichiometric release ratio), even an order of magnitude higher concentra-

tions would only lead to less than 1 kcal/mol increase in ΔG_r . We have no independent evidence of the critical value of ΔG_r for bytownite dissolution, however, the calculated experimental values are significantly below the critical value (-10 kcal/mol) found for the nearest analog, albite, by Burch et al. (1993), confirming the experimental conclusion that dissolution rates in these experiments were determined on the bytownite dissolution plateau.

4.2. Dissolution kinetics

An expression for feldspar dissolution rate at a constant temperature can be written as:

$$r = kf(a_{\text{H}^+}, I, \Delta G_r, L), \quad (2)$$

Table 3

Final concentrations of ions (μM), saturation indices ($\text{SI} = \log \text{IAP}/K$) with respect to homogenous dissolution of the primary bytownite and possible secondary phases. All calculations at $\text{pH} = 6$ and at air saturation, except where noted. ΔG_r is in Kcal/mol

Experiment ($^{\circ}\text{C}$)	Final experimental concentrations (μM)				Gibbsite	$\text{SiO}_2(\text{am})$	Kaolinite	Bytownite	
	Si	Al	Ca^{a}	Na	SI	SI	SI	SI	ΔG_r
<i>Distilled water^b</i>									
5	5.9	0.14 ^c	2.0	0.6 ^a		-2.34	-1.13	-15.18	-19.34
20	16.7	0.05 ^c	5.2	1.7 ^a		-2.02	-0.64	-12.90	-17.32
35	32.5	0.04 ^c	10.8	3.6 ^a		-1.86	-0.44	-11.16	-15.75
<i>1 mM KNO_3</i>									
5	5	0.16 ^c	1.7	0.6 ^a		-2.41	-1.27	-15.44	-19.67
20	16	0.05 ^c	5.3	1.8 ^a		-2.04	-0.68	-12.97	-17.41
35	31	0.05 ^c	10.3	3.4 ^a		-1.88	-0.48	-11.27	-15.91
<i>1 mM Na acetate</i>									
5	4.4	0.08 ^c	1.4	1000		-2.47	-1.39	-14.06	-17.91
20	16.2	0.02 ^c	5.4	1000		-2.04	-0.67	-11.54	-15.50
35	30.7	0.03 ^c	10.2	1000		-1.88	-0.49	-10.01	-14.13
<i>1 mM Na_2 oxalate</i>									
5	11	23	3.7	2000	-3.60	-2.07	-7.79	-19.21	-24.47
20	25	32	8.3	2000	-2.50	-1.85	-5.29	-15.43	-20.72
35	40	24	13.3	2000	-1.82	-1.77	-3.89	-12.94	-18.27
<i>1 mM Na gluconate</i>									
5	7	9	2.3	1000	0.34	-2.27	-0.29	-12.74	-16.23
20	18	5	6	1000	-0.65	-1.99	-1.88	-12.46	-16.73
35	28	2	9.3	1000	-1.66	-1.92	-3.89	-12.98	-18.32

^aConcentrations estimated on the basis of Si concentrations and bytownite stoichiometry.

^bFinal distilled water $\text{pH} \approx 6.5$.

^cNo dissolved Al detected: Gibbsite saturation assumed.

where feldspar dissolution rate (r) is dependent on an intrinsic rate constant (k), and functions of proton activity (or $\text{pH} = -\log a_{\text{H}^+}$), ionic strength (I), solution saturation state (or chemical affinity, ΔG_r) and ligand activity (L) (Lasaga et al., 1994). All of these terms have potential temperature dependencies. The experiments were conducted under conditions where the chemical affinity term can be neglected (see above), and the small differences between the results of the distilled water and KNO_3 experiments demonstrate that the effects of ionic strength can be neglected in these short-duration experiments. Therefore, only the pH and ligand effects are likely to influence the rates of dissolution and the temperature dependence of dissolution in these experiments.

Feldspar dissolution rate is a complex function of pH. Dissolution rates are lowest and approximately independent of pH in near neutral solutions (pH 5 to

8), and increase with both increasing and decreasing pH (Chou and Wollast, 1985; Blum and Lasaga, 1988; Brady and Walther, 1989). The pH dependence of dissolution rate can be empirically described, in the absence of chemical affinity, ionic strength or ligand effects, as (Drever and Vance, 1994):

$$r = f(a_{\text{H}^+}) = k_1 a_{\text{H}^+}^n + k_2 + k_3 a_{\text{OH}^-}^m, \quad (3)$$

where r is dissolution rate; k_1 , k_2 and k_3 are the rate constants in acidic, neutral and basic solutions; n and m are the order of the reaction and are related to the adsorption of protons and hydroxyl ions on the mineral surface (Blum and Lasaga, 1988; Brady and Walther, 1989). Our experiments were performed in neutral pH conditions (the pH range of most natural environments) where dissolution rates are lowest and

independent of small changes in pH. Therefore, in our experiments, the first and third terms in Eq. 3 should be negligible and the reaction rate, r , should be equal to k_2 (Hellmann, 1994). The distilled water and KNO_3 experiments provide the basis for estimating the temperature dependence of the rate constant for hydrolytic dissolution, k_2 . The remaining experiments provide the basis for determining the additional impact of ligands on the dissolution process and the temperature dependence of this additional process.

4.3. Apparent activation energies

Fig. 3 shows bytownite dissolution rates as a function of temperature in the different treatments. The apparent activation energies of dissolution fall into two groups (Table 1). The distilled water and KNO_3 experiments have apparent activation energies of approximately 10 kcal/mol. The apparent activation energy of bytownite dissolution determined in the acetate solutions, a ligand that forms only weak complexes with dissolved Al, is similarly ≈ 10 kcal/mol. Based on an analysis of covariance of all of the data in Table 1 (Sokal and Rohlf, 1981), the activation energies determined in these three experiments are indistinguishable ($P = 0.5$). The apparent activation energies of bytownite dissolution in solutions of oxalate and gluconate, both ligands that form strong complexes with dissolved Al and presumably at Al-sites on the bytownite surface, are also homogeneous ($P = 0.67$) but are significantly different from the other three experiments ($P = 0.0002$).

The overall rates of bytownite dissolution in our oxalate and gluconate experiments represent the net effect of the rates associated with hydrolysis and ligand-promoted dissolution (see Eq. 2). Although the exact nature of the interaction between the two reaction mechanisms is not clear and cannot be determined on the basis of these experiments alone, the impact of the ligand-promoted effect on the overall dissolution process is equivalent, in these experiments, to a 3 kcal/mol catalytic reduction in the apparent activation energy of bytownite dissolution.

The apparent activation energy for feldspar dissolution has been estimated previously in a number of laboratory and field studies (Brady, 1991; Brady and

Carroll, 1994; Velbel, 1993; Hellmann, 1994; Lasaga et al., 1994 and references therein; Dorn and Brady, 1995; Chen and Brantley, 1997). Knauss and Wolery (1986) calculated an E_a of 13 kcal/mol for albite dissolved in a flow-through reactor at neutral pH for a temperature range of 25°C to 70°C. Brady and Carroll (1994) calculated an E_a of 11.5 kcal/mol for Si release from labradorite feldspar in a flow-through reactor in slightly acidic solutions (pH 4) from 21°C to 60°C. Tole et al. (1986) obtained values of 12–15 kcal/mol for the dissolution nepheline, a feldspathoid, in neutral pH solutions from 25°C to 80°C. Hellmann (1994) determined an apparent activation energy of 16.5 kcal/mol for albite dissolution at neutral pH and temperatures between 100°C and 300°C. Chen and Brantley (1997) determined apparent energy for albite dissolution over a range of temperature and pH (up to 4.5) and calculated a value of 15.6 kcal/mol. In general, the E_a for silicate minerals dissolved at low temperatures and different experimental conditions ranges from 10 to 20 kcal/mol (Lasaga et al., 1994). The value obtained in this study for silica release, 10 kcal/mol, is in the lower end of the range for silicate minerals but is consistent with other values obtained for plagioclase feldspars at near neutral pH conditions.

Our activation energy estimates are based on a simple, proton and Al^{3+} -independent, kinetic model. A number of investigators (Carroll-Webb and Walther, 1988; Carroll and Walther, 1990; Casey and Sposito, 1992; Hellmann, 1994) have demonstrated that apparent activation energies may have pH dependence. Since our experiments were conducted at essentially constant pH, we cannot take this pH dependence into account in our calculations. Oelkers et al. (1994) have suggested that aluminosilicate dissolution rates may be dependent on Al^{3+} concentrations in solution. In our experiments with distilled water, KNO_3 , acetate and oxalate, free Al^{3+} concentrations were below analytical detection or fully complexed in solution. For the gluconate experiments, the speciation of Al^{3+} could not be determined analytically. However, equilibrium calculations, based on the data in Table 3, suggest that Al^{3+} concentrations would similarly be below our analytical detection. We, therefore, cannot consider the possibility of Al^{3+} -dependent kinetics and the impact of the Oelkers et al. (1994) kinetic formulation on

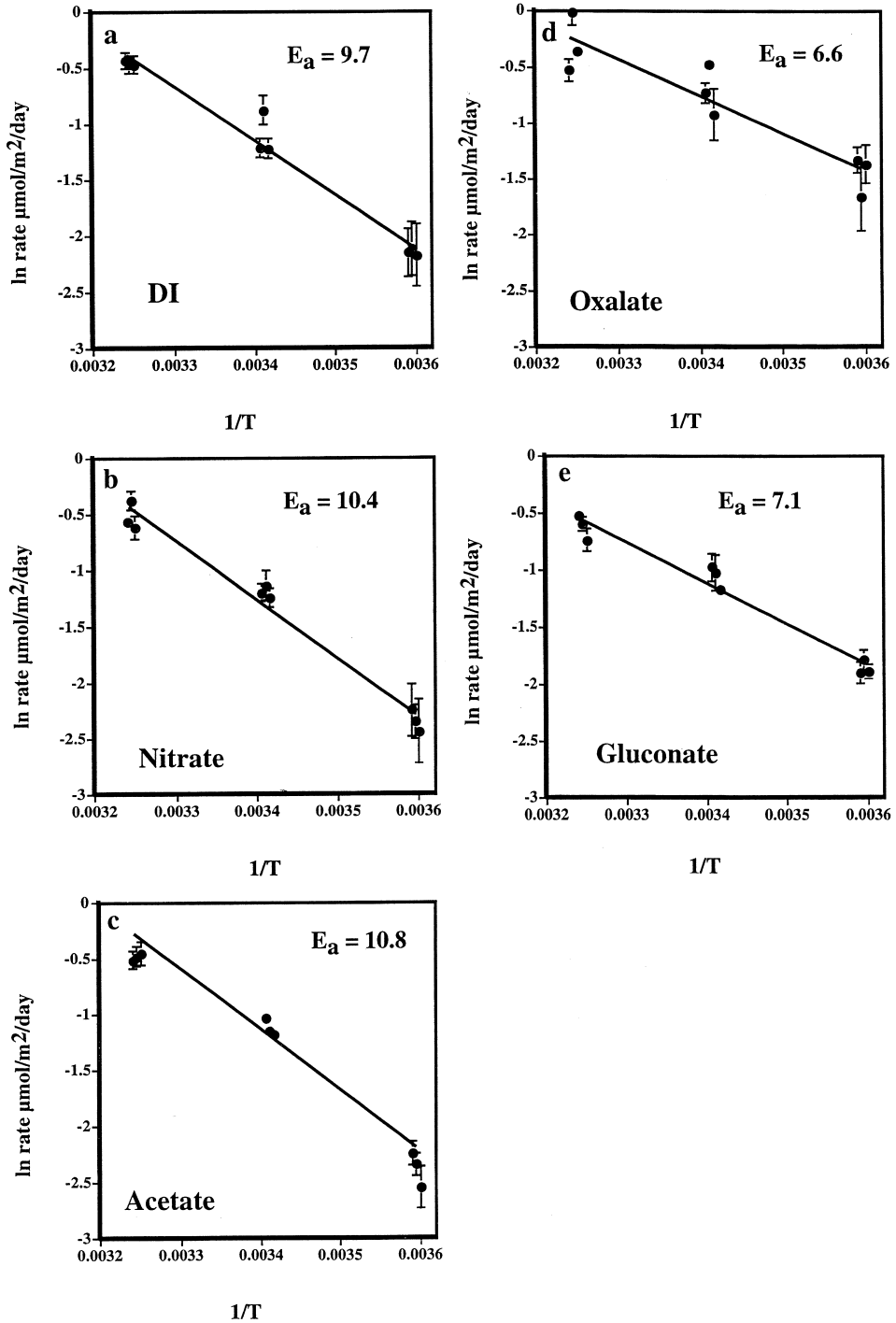


Fig. 3. Arrhenius plots for Si release from feldspar in (a) deionized water, (b) 1 mM KNO_3 , (c) 1 mM sodium acetate, (d) 1 mM sodium oxalate, (e) 1 mM sodium gluconate. Data points for replicate experiments are offset by ± 0.00005 along the x-axis.

our estimates of the temperature dependence of bytownite dissolution.

Higher values of E_a have been determined from field measurements of feldspar weathering rates. Dorn and Brady (1995) use backscattered electron microscopic images of plagioclase feldspar from Hawaiian volcanoes to determine the effects of temperature on weathering over long time scales. They chose sites that had similar rock types and similar environmental conditions (i.e., same amount of rainfall, no encrusting organisms), but different mean annual temperatures. The apparent activation energy determined from the extent of plagioclase feldspar weathering was 26.2 kcal/mol, much higher than the laboratory estimate of 10–15 kcal/mol. Velbel (1993) estimated plagioclase feldspar weathering rates from two catchments that had similar conditions (i.e., rock types, rainfall, soils, topography), but were at different elevations and, therefore, had different mean temperatures. The E_a for feldspar hydrolysis (based on Na release) is 18.4 kcal/mol, again higher than the laboratory estimates of E_a . Velbel (1993) attributes the anomalously low E_a in laboratory experiments to the artificially high weathering rates determined in the laboratory at low temperatures, which decrease the slope of the Arrhenius plot. This may be a factor in our experiments, since experiments lasted only a short time, a true long-term dissolution rate was not attained. However, the E_a of Na release from feldspar is not necessarily equal to the E_a of Al or Si release since these reactions all occur by different or a different series of mechanisms (Casey and Bunker, 1990). There are also uncertainties in the field measurements, such as uncertainties and variations in temperature, and small differences in topography, soils and vegetation, which also contribute to the discrepancies between laboratory and field measurements.

Part of the discrepancy between laboratory and field estimates of apparent activation energy of mineral dissolution may be due to the effects of seasonal temperature cycles. Field estimates of E_a are calculated from a mass flux of material from different areas, assuming an average mean temperature. However, since weathering rate is a logarithmic function of temperature, rates increase faster with an increase in temperature than they decrease for an equivalent decrease in temperature. The “kinetic mean temper-

ature” is always greater than the actual mean temperature and the apparent activation energies from field measurements overestimates the real temperature dependence of the dissolution reaction (Lasaga et al., 1994). Seasonal variations of rainfall and biological activity may also yield different apparent activation energies in field compared to laboratory experiments.

4.4. Stoichiometry

Feldspar dissolution in all of these experiments is nonstoichiometric over the temperature range tested. In the inorganic control and acetate experiments, silica was preferentially released to solution at all three temperatures compared to Al, which was below detection in all cases. However, Al was released to solution in the experiments with complexing organic acids, in most cases at a stoichiometric ratio above that of the dissolving mineral (Fig. 4). Similar results were obtained in previous feldspar dissolution experiments with this mineral in flow-through reactors in our laboratory (Welch and Ullman, 1993, 1996). Al/Si release ratios were lowest in neutral inorganic solutions and increased with increased acidity or organic ligand content. Several other laboratory and field studies on mineral weathering have demonstrated an increase in Al release to solution in the presence of complexing organic ligands (Antweiler and Drever, 1983; Surdam et al., 1984; Mast and Drever, 1987; Stillings et al., 1996).

Nonstoichiometric dissolution may be the result of preferential dissolution of a more siliceous phase, precipitation of secondary Al-rich phases or formation of a residual leached material (Casey and Bunker, 1990). It is unlikely that excess Si release is due primarily to the dissolution of a more Si-rich phase. Bulk feldspar from Crystal Bay contains traces of garnets, metal oxides and clays, most of which are removed by the physical and chemical sample pretreatment processes. In addition, Si-rich phases, such as quartz or more siliceous feldspars, which could be present in the treated sample, dissolve more slowly than bytownite and, therefore, cannot be responsible for the nonstoichiometry (Welch and Ullman, 1996).

Another possibility is that secondary phases, such as gibbsite, kaolinite or amorphous silica, are precipitating in the reactor. Our calculations (above and

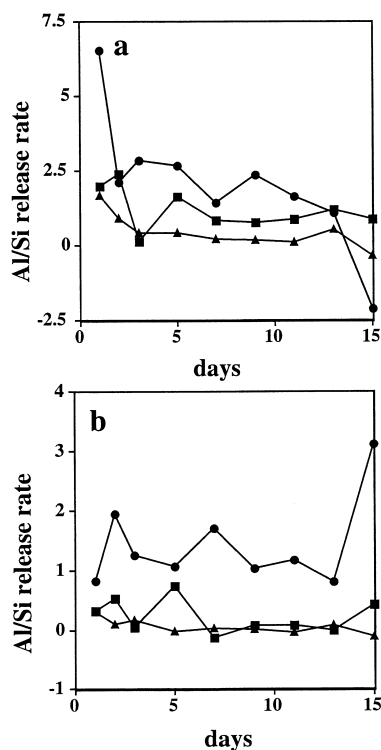


Fig. 4. Al/Si release rate for feldspar dissolved in (a) 1 mM oxalate and (b) 1 mM gluconate solutions at 5°C (●), 20°C (■) and 35°C (▲).

Table 3) indicate that none of the experimental solutions are supersaturated with these secondary phases when Al is detectable. It is possible that gibbsite solubility is controlling Al concentrations in the experimental solutions where Al was not detected and, therefore, could account for the observed nonstoichiometric dissolution in the inorganic or acetate experiments, but not for the excess Al concentrations and release found in the complexing ligand experiments. Another possibility is that a residual material is forming at mineral surfaces (Pačes, 1973; Chou and Wollast, 1984). However, the amount of material released to solution in these short-duration experiments is insufficient to account for substantial leached layer formation.

Oxalate enhanced Si release from minerals at all temperatures, but it was particularly effective in enhancing Si release at the lowest temperature (Table 1). Gluconate enhanced dissolution to a lesser

extent, but again the effect was greatest at the lowest temperature. This increase in Si release was correlated with Al release (Fig. 2d and e) and Al/Si release ratios (Fig. 4), indicating that the increase in Si release rates by oxalate or gluconate is controlled by the Al release. This probably occurs due to the decoordination of Si tetrahedra as Al is removed from the mineral surface (Brady and Walther, 1989). Several other studies have demonstrated an enhancement of aluminosilicate mineral dissolution due to oxalate (Surdam et al., 1984; Manley and Evans, 1986; Bennett et al., 1988; Bevan and Savage, 1989; Johnston and Vestal, 1993; Welch and Ullman, 1993). Microbial production of gluconate also enhances aluminosilicate mineral dissolution in batch reactors although gluconate was not as effective as oxalate at enhancing rates (Vandevivere et al., 1994). This catalytic effect is responsible for the ~3 kcal/mol difference in activation energies found in our two groups of experiments (see above).

Both oxalate and gluconate form bidentate inner-sphere complexes with aluminum and, therefore, should attack feldspar surfaces and participate in aluminosilicate mineral weathering reactions (Motekaitis and Martell, 1984; Fein, 1991). The stability constants for various Al-oxalate complexes in solution increase with increasing temperatures from 25°C to 100°C (Tait et al., 1992; Thyne et al., 1992). Therefore, it could be expected that Al complexing at surface sites and Al release to solution will increase with increasing temperatures. Given the similarity in ligand and complex structure, both oxalate and gluconate should follow the same trend. The predicted increase in Al-release rates with temperature, as suggested by the stability trend, however, did not occur in our experiments. Final Al concentration in oxalate solution increased with increasing temperatures from 5°C to 20°C but, then, concentration decreased as temperature increased to 35°C. The Al/Si release ratio in the oxalate experiments decreased with increasing temperatures from three to four times higher than the mineral stoichiometry at 5°C to approximately stoichiometric dissolution at 35°C (Fig. 4a). A similar trend was observed in the gluconate treatments, with Al/Si release ratios decreasing with increasing temperatures (Fig. 4b). Therefore, the temperature dependence of Al-ligand stability in solution cannot be the

primary factor controlling Al release rates in these batch experiments.

Since changes in the stability of Al–organic complexes in solution with temperature cannot account for the observations in these experiments, then other mineral–organic interactions must be controlling dissolution rates. There is little data on the temperature dependence of adsorption of low molecular weight organics to mineral surfaces. In one study, Fein and Brady (1995) found that the adsorption of oxalate to alumina surfaces did not change significantly from 25°C to 60°C, although, in general, adsorption of organics to surfaces decreases with increasing temperature (Afzal et al., 1990; Schwartzenbach et al., 1993; Piatt et al., 1996). The increase in adsorption at lower temperatures can be attributed to a decrease in the solubility of organic compounds as temperatures decrease and a negative enthalpy of sorption (Piatt et al., 1996). Some experiments have shown (Carroll and Walther, 1990; Brady and Walther, 1992; Hellmann, 1994; Chen and Brantley, 1997) that the pH dependence of dissolution rates increases with increasing temperature due to proton adsorption to the surface. At a given pH, with increasing temperature, proton adsorption was found to increase due to changes in mineral surface charge; conversely, anion adsorption should increase with decreasing temperature. As organic anion adsorption is an early step in the dissolution process, the enhancement of mineral dissolution due to organic interactions with the mineral surface should be reduced at higher temperatures. This is consistent with our results that show the largest relative enhancement of dissolution rates at low temperatures.

The stability of Al–organic complexes in solution or on alumina surfaces may not, however, be a good predictor of the reactions of Al–organic complexes on the feldspar surface. Kummert and Stumm (1980) determined that the tendency for organic ligands to form complexes with surface Al atoms on hydrous Al_2O_3 was similar to that of organic ligands to form complexes with Al^{+3} in solution. However, Al is octahedrally coordinated in solution and in alumina and tetrahedrally coordinated in feldspars, which may affect the interaction between the ligand and the Al ion or Al surface sites on the feldspar surface. Ligands may more easily bond directly to tetrahedrally coordinated Al atoms on the feldspar mineral surface

since the Al d-orbitals are empty and available to accept electron pairs. The formation of the complexed aluminum tetrahedron, particularly the formation of a bidentate complex, may be the important step in the conversion to the octahedral soluble form. The similarity in the E_a of bytownite dissolution in oxalate and gluconate solution suggests that oxalate and gluconate are similarly effective at catalyzing the tetrahedral Al to octahedral Al transition on the feldspar surface, although they differ substantially in the strength of the Al–organic complex in solution.

4.5. Implications for global weathering

The magnitude of the feedback between Ca–Mg–silicate mineral weathering and atmospheric CO_2 and global climate depends on the apparent activation energy of mineral dissolution, higher E_a values result in stronger negative feedback (Walker et al., 1981; Berner et al., 1983; Volk, 1987; Brady, 1991; Brady and Carroll, 1994). Berner (1993) used a value of 15 kcal/mol for E_a to estimate atmospheric CO_2 concentration and mean global temperature over geologic time. This model predicted a greater temperature variation than can be demonstrated based on paleoclimatic data. When higher values of E_a are used (20 kcal/mol), the model predicts both lower values of $p\text{CO}_2$ and smaller fluctuations in temperature over geologic time (Brady, 1991). The values of E_a determined in our experiments for the weathering of Ca-rich plagioclase feldspar would lead to a weaker feedback and larger excursions in atmospheric CO_2 and climate. It is unrealistic, however, to take our measured values of E_a and substitute them directly into these models as the dissolution reaction is only one component of the natural weathering process: the weathering mechanism may vary with temperature as well. The experimental temperature dependence of dissolution rate should not be used alone as a proxy for the temperature dependence of natural mineral weathering. Nonetheless, our results are consistent with observations of naturally weathered rocks and can have implications for seasonal weathering fluxes or the role of biologically mediated weathering over a range of temperature.

Observations of naturally weathered rock surfaces from a Hawaiian lava flow demonstrate that lichen-mediated rock-weathering rates are faster than for

uncolonized surfaces by a factor of approximately 2 to 20, though rates varied as a function of temperature and precipitation (Dorn and Brady, 1995; Brady et al., 1999). The apparent activation energy for lichen-mediated weathering of plagioclase and olivine was approximately 12 kcal/mol, significantly lower than the 20 to 26 kcal/mol for abiotic weathering of similar rock surfaces. This is consistent with our experimental work, which demonstrates the catalytic effect of organically mediated mineral dissolution. Although the absolute increase in the rate of mineral dissolution and of natural weathering increases with temperature, the relative increase, $r_{\text{organic}}/r_{\text{inorganic}}$, is actually greatest at the lowest temperature and, therefore, biologically mediated silicate weathering reactions at low temperatures might be more important than previously suspected. Johnston and Vestal (1993), for example, have shown strikingly high rates of mineral weathering associated with oxalate production by lichens in Antarctic soils.

The interesting corollary to this is that, as temperatures increase, organic ligands should have a lesser effect on catalysis of the dissolution reaction, and at some temperature, the rates of organically mediated and hydrolytic silicate mineral dissolution far from equilibrium should be indistinguishable. This occurs at approximately 35°C for gluconate (Table 1 and Fig. 4) and at $\approx 60^\circ\text{C}$ for oxalate (estimated by extrapolation). This does not mean, however, that at higher temperatures, these ligands have no effect on silicate mineral weathering reaction. They still may be able to affect dissolution by indirect means. Since the stability constant of Al–organic complexes tend to increase with temperature, these ligands should be particularly effective in increasing the overall amount of material released to solution and the rates of dissolution closer to equilibrium. This effect may be less dramatic, but still important, in many geological settings.

Even though feldspars are the most abundant mineral at the Earth's surface, their weathering rates and temperature dependence of weathering rate are generally lower than for other less stable Ca- and Mg-silicates (Lasaga et al., 1994; Chen and Brantley, 1998). For example, the dissolution rates of two Ca–Mg-rich pyroxenes, enstatite and diopside, determined in laboratory experiments, are approximately two orders of magnitude faster than the dissolution

rate for feldspars under similar experimental conditions (Lasaga et al., 1994 and references therein). The experimentally determined temperature dependence of pyroxene dissolution is also larger than for feldspars (approximately 20 kcal/mol). Therefore, the chemical weathering of other Ca–Mg-silicate minerals (such as pyroxenes, amphiboles and olivine) may be a more available source of Ca and Mg to solution and, consequently, a more important regulator of atmospheric CO_2 than the weathering of the more abundant feldspars.

In addition, other biologically mediated processes may affect weathering rate and, therefore, the temperature dependence of weathering. For example, as temperatures increase due to higher atmospheric CO_2 , biomass should also increase due to higher photosynthesis rates. Increasing plant abundance due to increased temperature and atmospheric CO_2 concentrations should cause increased production of soil CO_2 and organic acids (Volk, 1987; Berner, 1991; Gwiazda and Broecker, 1994). The rates of production of these dissolution-enhancing compounds should increase with temperature due to higher metabolic rates.

5. Conclusions

The apparent activation energy for hydrolytic Si release from bytownite feldspar determined in our experiments is approximately 10 kcal/mol. This value is in the lower end of the range for E_a of other silicate minerals (10–20 kcal/mol), but it is consistent with other laboratory measurements of feldspar dissolution. Acetate, a ligand that forms only weak complexes with Al in solution and presumably at the Al-sites at the mineral surface, has no effect on mineral dissolution and the temperature dependence of dissolution. Both oxalate and gluconate, ligands that form strong bidentate complexes with Al in solution, enhanced dissolution by catalyzing the release of Al from the mineral surface. The catalysis leads to a decrease in the activation energy of dissolution of approximately 3 kcal/mol. These compounds had a relatively larger effect on dissolution rates at lower temperatures, presumably due to an increase in the adsorption of these compounds to the

Al-sites at the mineral surface, an early step in the dissolution process.

Acknowledgements

This work was supported by a grant to W.J.U. from the US Department of Energy Subsurface Science Program (Dr. F. Wobber, Program Director). The authors benefited from a number of reviews of this manuscript, including the comments of J. Walther, B. Saylor, S. Brantley, J. Fein and D. Schwartzman.

References

- Afzal, M., Hamdani, K., Ahmad, H., 1990. Thermodynamics of adsorption of organic acids from aqueous solutions on neutral alumina. *Sci. Int.* 2, 101–106.
- Antweiler, R.C., Drever, J.I., 1983. The weathering of a late tertiary volcanic ash: importance of organic solutes. *Geochim. Cosmochim. Acta* 47, 623–629.
- Bennett, P.C., Melcer, M.E., Siegel, D.I., Hassett, J.P., 1988. The dissolution of quartz in dilute aqueous solutions of organic acids at 25°C. *Geochim. Cosmochim. Acta* 52, 1521–1530.
- Berner, R.A., 1991. Model for atmospheric CO₂ over Phanerozoic time. *Am. J. Sci.* 291, 339–376.
- Berner, R.A., 1993. Paleozoic atmospheric CO₂: importance of solar radiation and plant evolution. *Science* 261, 68–70.
- Berner, R.A., Holdren, G.R. Jr., 1979. Mechanism of feldspar weathering: II. Observations of feldspars from soils. *Geochim. Cosmochim. Acta* 43, 1173–1186.
- Berner, R.A., Lasaga, A.C., Garrels, R.M., 1983. The carbon-silicate geochemical cycle and its effect on atmospheric carbon dioxide over the past 100 million years. *Am. J. Sci.* 283, 641–683.
- Bevan, J., Savage, D., 1989. The effect of organic acids on the dissolution of K-feldspar under conditions relevant to burial diagenesis. *Mineral. Mag.* 53, 415–425.
- Blum, A., Lasaga, A.C., 1988. Role of surface speciation in the low temperature dissolution of minerals. *Nature* 331, 431–433.
- Bottari, E., Ciavatta, L., 1968. Studio potentiometrico dei complessi Al(III)-ossalato. *Gazz. Chim. Ital.* 98, 1004–1013.
- Brady, P.V., 1991. The effect of silicate weathering on global temperature and atmospheric CO₂. *J. Geophys. Res.* 96, 18101–18106.
- Brady, P.V., Dorn, R.I., Brazel, A.J., Clark, J., Moore, R.B., Glidewell, T., 1999. Direct measurement of the combined effects of lichen, rainfall, and temperature on silicate weathering. *Geochim. Cosmochim. Acta* 63, 3293–3300.
- Brady, P.V., Carroll, S.A., 1994. Direct effects of CO₂ and temperature on silicate weathering: possible implications for climate control. *Geochim. Cosmochim. Acta* 58, 1853–1856.
- Brady, P.V., Walther, J.V., 1989. Controls on silicate dissolution rates in neutral and basic pH solutions at 25°C. *Geochim. Cosmochim. Acta* 53, 2823–2830.
- Brady, P.V., Walther, J.V., 1992. Surface chemistry and silicate dissolution at elevated temperatures. *Am. J. Sci.* 292, 639–658.
- Burch, T.E., Nagy, K.L., Lasaga, A.C., 1993. Free energy dependence of albite dissolution kinetics at 80°C and pH 8.8. *Chem. Geol.* 105, 137–162.
- Carroll, S.A., Walther, J.V., 1990. Kaolinite dissolution at 25°, 60°, and 80°C. *Am. J. Sci.* 290, 797–810.
- Carroll-Webb, S.A., Walther, J.V., 1988. A surface complexation model for the pH dependence of corundum and kaolinite dissolution rates. *Geochim. Cosmochim. Acta* 52, 2609–2623.
- Casey, W.H., Bunker, B., 1990. Leaching of mineral and glass surfaces during dissolution. In: *Mineral–Water Interface Geochemistry*. Hochella, M.F., White, A.F. (Eds.), Rev. Mineral. 23 Mineralogical Society of America, pp. 397–426.
- Casey, W.H., Sposito, G., 1992. On the temperature dependence of mineral dissolution rates. *Geochim. Cosmochim. Acta* 56, 3825–3830.
- Chen, Y., Brantley, S.L., 1997. Temperature and pH dependence of albite dissolution rate at acid pH. *Chem. Geol.* 135, 275–290.
- Chen, Y., Brantley, S.L., 1998. Diopside and anthophyllite dissolution at 25° and 90°C and acid pH. *Chem. Geol.* 147, 233–248.
- Chou, L., Wollast, R., 1984. Study of the weathering of albite at room temperature and pressure with a fluidized bed reactor. *Geochim. Cosmochim. Acta* 48, 2205–2217.
- Chou, L., Wollast, R., 1985. Steady-state kinetics and dissolution mechanisms of albite. *Am. J. Sci.* 285, 963–993.
- Dorn, R.I., Brady, P.V., 1995. Rock-based measurement of temperature dependent plagioclase weathering. *Geochim. Cosmochim. Acta* 59, 2847–2852.
- Drever, J.I., Vance, G.F., 1994. Role of soil organic acids in mineral weathering processes. In: Pittman, E.D., Lewan, M.D. (Eds.), *Organic Acids in Geological Processes*. Springer, New York, pp. 138–161.
- Eggleston, C.M., Hochella, M.F. Jr., Parks, G.A., 1989. Sample preparation and aging effects on the dissolution rate and surface composition of diopside. *Geochim. Cosmochim. Acta* 53, 797–804.
- Fein, J.B., 1991. Experimental study of aluminum-oxalate complexing at 80°C: implications for the formation of secondary porosity within sedimentary reservoirs. *Geology* 19, 1037–1040.
- Fein, J.B., Brady, P.V., 1995. Mineral surface controls on the diagenetic transport of oxalate and aluminum. *Chem. Geol.* 121, 11–18.
- Fisher, J.B., 1987. Distribution and occurrence of aliphatic acid anions in deep subsurface waters. *Geochim. Cosmochim. Acta* 51, 2459–2468.
- Fox, T.R., Comerford, N.B., 1990. Low-molecular-weight organics in selected forest soils of the southeastern USA. *Soil Sci. Soc. Am. J.* 54, 1139–1144.
- Franklin, S.P., Hajash, A. Jr., Dewers, T.A., Tieh, T.T., 1994. The role of carboxylic acids in albite and quartz dissolution: an

- experimental study under diagenetic conditions. *Geochim. Cosmochim. Acta* 58, 4259–4279.
- Gordienko, V.I., Mikhailuk, Y.I., 1970. Indicator amperometric method for determining instability constants of very simple complexes: Communication 1. Non-protonated complexes. *Zh. Anal. Khim.* 25, 2267.
- Graustein, W.C., Cromack, K. Jr., Sollins, P., 1977. Calcium oxalate: occurrence in soils and effect on nutrient and geochemical cycles. *Science* 198, 1252–1254.
- Gwiazda, R.H., Broecker, W.S., 1994. The separate and combined effects of temperature, soil $p\text{CO}_2$, and organic acidity on silicate weathering in the soil environment: formulation of a model and results. *Global Biogeochem. Cycles* 8, 141–155.
- Hellmann, R., 1994. The albite–water system: Part I. The kinetics of dissolution as a function of pH at 100, 200, and 300°C. *Geochim. Cosmochim. Acta* 58, 595–611.
- Holdren, G.R. Jr., Addams, J.E., 1982. Parabolic dissolution kinetics of silicate minerals: an artifact of nonequilibrium precipitation processes? *Geology* 10, 186–190.
- Jaber, M., Bertin, F., Thomas-David, G., 1977. Application of infrared and Raman spectroscopy and nuclear magnetic resonance in study of complexes in aqueous solution, $\text{Al}^{+3} - \text{H}_2\text{C}_2\text{O}_4$. *Can. J. Chem.* 55, 3689–3699.
- Johnston, C.G., Vestal, J.R., 1993. Biogeochemistry of oxalate in Antarctic cryptoendolithic lichen-dominated community. *Microb. Ecol.* 25, 305–319.
- Knauss, K.G., Wolery, T.J., 1986. Dependence of albite dissolution kinetics on pH and time at 25°C and 70°C. *Geochim. Cosmochim. Acta* 50, 2481–2498.
- Kummert, R., Stumm, W., 1980. The surface complexation of organic acids on hydrous $\delta\text{-Al}_2\text{O}_3$. *J. Colloid Interface Sci.* 75, 373–385.
- Lasaga, A.C., Soler, J.M., Ganor, J., Burch, T., Nagy, K.L., 1994. Chemical weathering rate laws and global geochemical cycles. *Geochim. Cosmochim. Acta* 58, 2361–2386.
- Lowell, S., Shields, J.E., 1984. *Powder Surface Area and Porosity*. Chapman & Hall, New York, 234 pp.
- Manley, E.P., Evans, L.J., 1986. Dissolution of feldspars by low-molecular-weight aliphatic and aromatic acids. *Soil Sci.* 141, 106–112.
- Masone, M., Vicedomini, M., 1981. Gluconate and lactate as ligands of calcium ion. *Anal. Chem. (Rome)* 71, 517–523.
- Mast, M.A., Drever, J.I., 1987. The effect of oxalate on the dissolution rates of oligoclase and tremolite. *Geochim. Cosmochim. Acta* 51, 2559–2568.
- Motekaitis, R.J., Martell, A.E., 1984. Complexes of aluminum(III) with hydroxy carboxylic acids. *Inorg. Chem.* 23, 18–23.
- Nagy, K.L., Blum, A.E., Lasaga, A.C., 1991. Dissolution and precipitation kinetics of kaolinite at 80°C and pH 3: the dependence on solution saturation state. *Am. J. Sci.* 291, 649–686.
- Nagy, K.L., Lasaga, A.C., 1992. Dissolution and precipitation kinetics of gibbsite at 80°C and pH 3: the dependence on solution saturation state. *Geochim. Cosmochim. Acta* 56, 2903–3111.
- Nordstrom, D.K., May, H.M., 1996. Aqueous equilibrium data for mononuclear aluminum species. In: Sposito, G. (Ed.), *The Environmental Chemistry of Aluminum*. 2nd edn. Lewis Publishers, Boca Raton, FL, pp. 39–80.
- Oelkers, E.H., Schott, J., Devidal, J.L., 1994. The effect of aluminum, pH, and chemical affinity on the rates of aluminosilicate dissolution reactions. *Geochim. Cosmochim. Acta* 58, 661–669.
- Pačes, T., 1973. Steady-state kinetics and equilibrium between ground water and granitic rock. *Geochim. Cosmochim. Acta* 37, 2641–2663.
- Palmer, D.A., Bell, J.L.S., 1994. Aluminum speciation and equilibria in aqueous solution: IV. A potentiometric study of aluminum acetate complexation in acidic NaCl brines to 150°C. *Geochim. Cosmochim. Acta* 58, 651–659.
- Parkhurst, D.L., 1995. *User's Guide to PHREEQC — A Computer Program for Speciation, Reaction-Path, Advective-Transport, and Inverse Geochemical Calculations*. Water-Resources Investigation Report 95-4227. US Geological Survey, Lakewood, CO, 143 pp.
- Piatt, J.J., Backhus, D.A., Capel, P.D., Eisenreich, S.J., 1996. Temperature-dependent sorption of naphthalene, phenanthrene, and pyrene to low organic carbon aquifer sediments. *Environ. Sci. Technol.* 30, 751–760.
- Schwartzbach, R.P., Gschwend, P.M., Imboden, D.M., 1993. *Environmental Organic Chemistry*. Wiley, New York, 681 pp.
- Sjöberg, S., Öhman, L.-O., 1985. Equilibrium and structural studies of silicon (IV) and aluminum (III) in aqueous solution: XIII. A potentiometric and 27 Al nuclear magnetic resonance study of speciation and equilibria in the aluminum (III)–oxalic acid–hydroxide system. *J. Chem. Soc., Dalton Trans.*, 2665–2669.
- Smith, R.M., Martell, A.E., 1993. *NIST Critical Stability Constants of Metal Complexes Database (Version 1.0)*. National Institute of Standards and Technology, Gaithersburg, MD. (September 1993) (Electronic compilation).
- Sokal, R.R., Rohlf, F.J., 1981. *Biometry*. 2nd edn. Freeman, New York, 859 pp.
- Stillings, L.L., Brantley, S.L., 1995. Feldspar dissolution at 25°C and pH 3: reaction stoichiometry and the effect of cations. *Geochim. Cosmochim. Acta* 59, 1483–1496.
- Stillings, L.L., Drever, J.I., Brantley, S.L., Sun, Y., Oxburgh, R., 1996. Rates of feldspar dissolution at pH 3–7 with 0–8 mM oxalic acid. *Chem. Geol.* 132, 79–89.
- Surdam, R.C., Boese, S.W., Crossey, L.J., 1984. The chemistry of secondary porosity. In: *Clastic Diagenesis*. McDonald, D.A., Surdam, R.C. (Eds.), *Am. Assoc. Pet. Geol. Mem.* 37 pp. 127–149.
- Tait, C.D., Janecky, D.R., Clark, D.L., Bennett, P.C., 1992. Oxalate complexation with aluminum (III) and iron (III) at moderately elevated temperatures. In: Kharaka, Y.K., Maest, A.S. (Eds.), *Water–Rock Interaction Volume 1 Low Temperature Environments*. Proceedings of the 7th International Symposium on Water–Rock Interaction, Park City, Utah, USA, 13–18 July. A.A. Balkema, Rotterdam, pp. 349–352.
- Thyne, G.D., Harrison, W.J., Alloway, M.D., 1992. Experimental study of the stability of the Al–oxalate complexation at 100°C and calculations of the effects of complexation on clastic diagenesis. In: Kharaka, Y.K., Maest, A.S. (Eds.), *Water–Rock*

- Interaction Volume 1 Low Temperature Environments. Proceedings of the 7th International Symposium on Water–Rock Interaction, Park City, Utah, USA, 13–18 July. A.A. Balkema, Rotterdam, pp. 353–357.
- Tole, M.P., Lasaga, A.C., Pantano, C., White, W.B., 1986. The kinetics of dissolution of nepheline ($\text{NaAlSi}_3\text{O}_8$). *Geochim. Cosmochim. Acta* 56, 845–850.
- Ullman, W.J., Kirchman, D.L., Welch, S.A., Vandevivere, P., 1996. Laboratory evidence for the microbially mediated silicate mineral dissolution in nature. *Chem. Geol.* 132, 11–17.
- Vandevivere, P., Welch, S.A., Ullman, W.J., Kirchman, D.L., 1994. Enhanced dissolution of silicate minerals by bacteria at near-neutral pH. *Microb. Ecol.* 27, 241–251.
- Velbel, M.A., 1993. Temperature dependence of silicate weathering in nature: how strong a negative feedback on long-term accumulation of atmospheric CO_2 and global greenhouse warming? *Geology* 21, 1059–1062.
- Volk, T., 1987. Feedbacks between weathering and atmospheric CO_2 over the last 100 million years. *Am. J. Sci.* 287, 763–779.
- Walker, C.G., Hays, P.B., Kasting, J.F., 1981. A negative feedback mechanism for the long-term stabilization of Earth's surface temperature. *J. Geophys. Res.* 86, 9776–9782.
- Welch, S.A., 1996. Effect of bacteria and microbial metabolites on bytownite feldspar dissolution at earth's surface temperature. PhD dissertation, Univ. of Delaware, 313 pp.
- Welch, S.A., Ullman, W.J., 1993. The effect of organic acids on plagioclase dissolution rates and stoichiometry. *Geochim. Cosmochim. Acta* 57, 2725–2736.
- Welch, S.A., Ullman, W.J., 1996. Feldspar dissolution in acidic and organic solutions: compositional and pH dependence of dissolution rate. *Geochim. Cosmochim. Acta* 60, 2939–2948.
- Welch, S.A., Ullman, W.J., 1999. The effect of microbial glucose metabolism on bytownite feldspar dissolution rates between 5 and 35°C. *Geochim. Cosmochim. Acta* 63, 3247–3259.
- Wogelius, R.A., Walther, J.V., 1991. Olivine dissolution at 25°C: effects of pH, CO_2 , and organic acids. *Geochim. Cosmochim. Acta* 55, 943–954.